JCB Article

# Mps3p is a novel component of the yeast spindle pole body that interacts with the yeast centrin homologue Cdc31p

**Sue L. Jaspersen, Thomas H. Giddings, Jr., and Mark Winey**

Department of Molecular, Cellular, and Developmental Biology, University of Colorado, Boulder, CO 80309

Accurate duplication of the *Saccharomyces cerevisiae* spindle pole body (SPB) is required for formation of a bipolar mitotic spindle. We identified mutants in SPB assembly by screening a temperature-sensitive collection of yeast for defects in SPB incorporation of a fluorescently marked integral SPB component, Spc42p. One SPB assembly mutant contained a mutation in a previously uncharacterized open reading frame that we call *MPS3* (for monopolar spindle). *mps3-1* mutants arrest in mitosis with monopolar spindles at the nonpermissive temperature, suggesting a defect in SPB duplication. Execution point experiments revealed that *MPS3* function is required for the first step of SPB duplication in G1. Like cells containing mutations in two other genes required for this step of SPB duplication (*CDC31* and *KAR1*), *mps3-1* mutants arrest with a single unduplicated SPB that lacks an associated half-bridge. *MPS3* encodes an essential integral membrane protein that localizes to the SPB half-bridge. Genetic interactions between *MPS3* and *CDC31* and binding of Cdc31p to Mps3p in vitro, as well as the fact that Cdc31p localization to the SPB is partially dependent on Mps3p function, suggest that one function for Mps3p during SPB duplication is to recruit Cdc31p, the yeast centrin homologue, to the half-bridge.

## Introduction

The spindle pole body (SPB)* is the *Saccharomyces cerevisiae* centrosome equivalent organelle. Organization of cytoplasmic microtubules by the SPB is needed for proper nuclear positioning, spindle orientation, and karyogamy, whereas nucleation of nuclear microtubules by the SPB is required for assembly of the mitotic spindle. Duplication of the SPB once, and only once, during each cell cycle is essential for formation of a bipolar mitotic spindle and accurate chromosome segregation. Yeast cells that fail to properly duplicate the SPB transiently arrest in mitosis due to the spindle checkpoint, which monitors the integrity of the mitotic spindle. However, because these cells are unable to repair the spindle defect, they will frequently undergo aberrant chromosome segregation due to a monopolar spindle, resulting in polyploid and aploid cells (Chial and Winey, 1999). Although faithful SPB duplication is essential for mitosis, very little is known about the mechanism and regulation of this process.

The SPB is a multilayered cylindrical structure that is embedded in the nuclear envelope throughout cell division (Byers and Goetsch, 1975). Thin section EM revealed that SPBs consist of three distinct layers: a central plaque within the plane of the nuclear membrane; an outer plaque facing the cytoplasm; and an inner plaque facing the nucleoplasm. In addition, one side of the SPB is associated with an electron-dense region of the nuclear envelope called the half-bridge (Byers and Goetsch, 1974). More recent analysis of SPB structure by electron tomography and cryo-EM have confirmed the presence of these three SPB substructures and have suggested that two intermediate layers connect the central plaque to the outer plaque (Bullitt et al., 1997; O'Toole et al., 1999).

Structural components of the SPB have been identified both genetically and biochemically, and the arrangement of proteins within the organelle has been determined by a combination of two-hybrid and immuno-EM analysis (Wigge et al., 1998; Adams and Kilmartin, 2000; Schramm et al., 2001). Important to this study is the central plaque component Spc42p and one of its binding partners, Spc29p, as well as the yeast centrin homologue Cdc31p, which binds a membrane protein of the half-bridge, Kar1p (Baum et al., 1986; Spang et al., 1993; Biggins and Rose, 1994; Vallen et al., 1994; Spang et al., 1995; Donaldson and Kilmartin,

Address correspondence to Mark Winey, MCD Biology, UCB 347, University of Colorado, Boulder, CO 80309-0347. Tel.: (303) 492-3409. Fax: (303) 492-7744. E-mail: mark.winey@colorado.edu

*Abbreviations used in this paper: SPB, spindle pole body; ts, temperature sensitive.

Key words: budding yeast; spindle pole body; *MPS3*; *CDC31*; centrin

1996; Bullitt et al., 1997; Adams and Kilmartin, 1999; Elliott et al., 1999).

SPB duplication proceeds via a discrete series of intermediates that have been characterized by EM analysis (for review see Adams and Kilmartin, 2000). During the G1 phase of the cell cycle, a small satellite structure containing Spc42p, Spc29p, Nud1p, and Cmn67p assembles at the distal end of the half-bridge on its cytoplasmic face. Next, the satellite enlarges, presumably due to templated assembly of Spc42p, to form the duplication plaque. Beneath the duplication plaque, the half-bridge elongates and fuses via an unknown mechanism. Assembly of the SPB is completed in late G1 when the half-bridge retracts, allowing the duplication plaque to be inserted into the nuclear envelope where it can associate with additional SPB components that make up the inner plaque.

Analysis of SPB structure in SPB duplication mutants has defined three distinct steps in the pathway (see Fig. 8 A). Mutations in *CDC31* and *KAR1*, which encode components of the half-bridge, cause a block early in SPB duplication before satellite deposition, resulting in cells with a single enlarged SPB lacking an associated half-bridge (Byers, 1981; Rose and Fink, 1987). The next step in SPB duplication is expansion of the satellite into the duplication plaque and is defined by mutants in *SPC42*, *SPC29*, and *MPS1*, an essential protein kinase (Winey et al., 1991; Donaldson and Kilmartin, 1996; Elliott et al., 1999). Cells with mutations in these genes also arrest with a single SPB. However, their function in SPB duplication can be separated from that of Cdc31p and Kar1p; they are required for SPB duplication after the mating pheromone arrest point in G1. Insertion of the duplication plaque into the nuclear envelope is the last genetically defined step of SPB duplication, and mutants in this step arrest in mitosis with duplicated SPBs, but the nascent SPB is not inserted into the nuclear envelope (Winey et al., 1991, 1993; Schutz and Winey, 1998).

To better understand the SPB duplication process, we identified putative mutants in SPB duplication using a novel SPB assembly assay in vivo. Genetic characterization of one of these mutants, *mps3-1* (monopolar spindle), revealed a function at the SPB. We show that *mps3-1* mutants arrest at the nonpermissive temperature in mitosis as large budded cells that contain a single, unduplicated SPB lacking any recognizable half-bridge structure. *MPS3* is an essential gene encoding an integral membrane protein that localizes to the half-bridge region of the SPB throughout the cell cycle. Mps3p genetically and physically interacts with Cdc31p, suggesting that one function of Mps3p in SPB duplication is recruitment of Cdc31p to the half-bridge. Consistent with this possibility, we found that Cdc31p localization to the SPB depends in part on Mps3p function.

## Results

### SPB assembly assay

We developed an SPB assembly assay in vivo to study the mechanism of SPB duplication. Overproduction of Spc42p results in lateral expansion of the central layer of the SPB (Donaldson and Kilmartin, 1996), and recently it was shown that this assembly depends on at least one known regulator of SPB duplication, *MPS1* (Castillo et al., 2002). To develop a direct, qualitative assay to measure Spc42p incorporation into the SPB, we constructed a strain containing a single integrated copy of *SPC42* fused at its COOH terminus to GFP (*SPC42–GFP*) under the control of the *GAL1/10* promoter. After a brief induction of *SPC42–GFP* expression by the addition of galactose (70 min), we analyzed the assembly of Spc42p–GFP into the SPB by epifluorescence microscopy. We found that wild-type cells incorporated Spc42p–GFP into the SPB at all cell cycle stages (Fig. 1 A; data not shown). Although prolonged overexpression of Spc42p results in a cell cycle arrest (Donaldson and Kilmartin, 1996), the short galactose induction used in our experiments did not result in accumulation of large amounts of Spc42p, and cells remained asynchronous (unpublished data). Consistent with previous

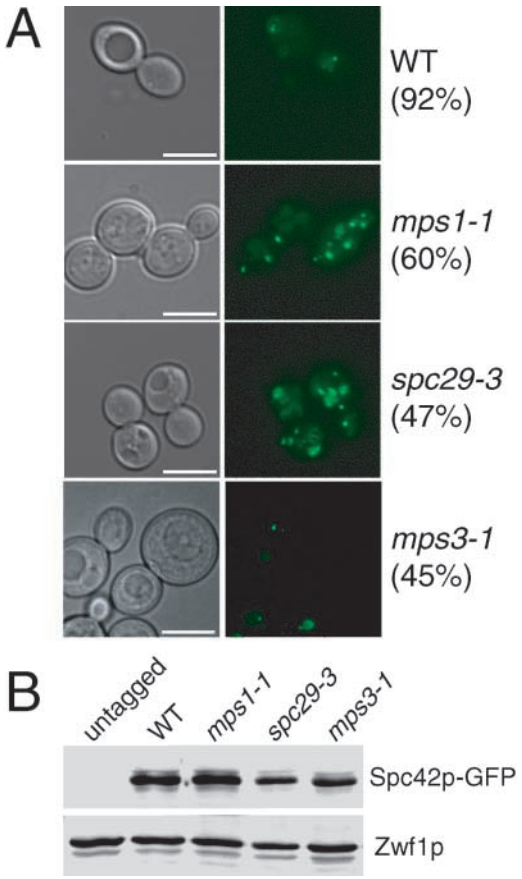


Figure 1. **Incorporation of Spc42p–GFP into the SPB depends on the function of Mps1p, Spc29p, and Mps3p.** Wild-type (SLJ761), *mps1-1* (SLJ753), *spc29-3* (SLJ756), and *mps3-1* (SLJ859) strains containing *GAL–SPC42–GFP* were grown to mid-log phase in media containing 2% raffinose at 23°C. After a 30-min shift to 34°C, galactose was added to a 1% final concentration to each culture to induce Spc42p–GFP expression. (A) Cells were analyzed for incorporation of Spc42p–GFP into the SPB by microscopy 70 min after addition of galactose. Wild-type cells incorporate Spc42p–GFP into the SPB in 92% of cells, whereas only 60% of *mps1-1* and 45% of *mps3-1* incorporate Spc42p–GFP into the SPBs. Although 47% of *spc29-3* cells incorporate Spc42p–GFP into the SPB, 46% of the cells exhibit multiple Spc42p–GFP signals per cell (speckles). Speckles were also observed in some *mps1-1* and *mps3-1* cells. Greater than 200 cells were counted in each sample. Bars, 5 μm. (B) Lysates were also prepared and analyzed for Spc42p–GFP production by Western blotting with anti-GFP antibodies (top). Zwf1p (glucose-6-phosphate dehydrogenase) serves as a loading control (bottom).

Table I. **Summary of mutants isolated in SPB assembly screen**

| Mutant No. | No. alleles isolated | Complementing ORF[b] | Gene | Confirmation method[a] | Null phenotype | Function |
|---|---|---|---|---|---|---|
| 99 | 1 | YJL018W and YJL019W | *MPS3* | L, PR, FC | inviable | SPB duplication (this study) |
| 157 | 1 | YER155C | *BEM2* | L, PR, FC | ts | Rho GTPase activating protein |
| 364/643 | 2 | YNL251C | *NRD1* | PR, FC | inviable | RNA recognition motif–containing protein |
| 419 | 1 | YGL073W | *HSF1* | PR, FC | inviable | Heat shock transcription factor |
| 745 | 1 | YCR042C | *TSM1* | L, PR, FC | inviable | TATA binding protein–associated factor |

[a]To verify that a mutation in the indicated ORF was responsible for the SPB assembly defect and the ts phenotype, the following tests were used: L, linkage between chromosomal marker and our ts mutation; PR, plasmid rescue of the growth defect of our ts mutation by isolated ORF; and FC, failure of deletion mutant to complement the ts phenotype of our mutant in a heterozygous diploid.
[b]ORF information was extracted from the *S. cerevisiae* Genome Database (Ball et al., 2000).

work, we demonstrated that Spc42p–GFP assembly into the SPB in our assay requires the function of *MPS1* (Castillo et al., 2002). *mps1-1* mutants shifted to the nonpermissive temperature for 30 min before galactose induction expressed Spc42p–GFP at wild-type levels, however the protein rarely appeared as two discrete foci of SPB signal, as was observed in wild-type cells (Fig. 1). Instead, multiple Spc42p–GFP foci were seen in 60% of cells, and in ~30% of cells, no Spc42p–GFP signal was detected (unpublished data). Using this assay, we found that assembly of Spc42p–GFP into the SPB also depends on the function of another protein required for SPB duplication, Spc29p (Fig. 1 A) (Adams and Kilmartin, 1999; Elliott et al., 1999). The requirement for Mps1p and Spc29p in our assay suggests that assembly of Spc42p–GFP into the SPB after its overexpression occurs through a similar pathway used for SPB duplication in G1 and is a method to analyze the genetic requirements for SPB duplication.

## SPB assembly screen

We reasoned that mutants in SPB assembly should be readily identifiable in a microscopic screen. We constructed a collection of 755 temperature-sensitive (ts) mutants in a yeast strain containing *GAL–SPC42–GFP*. To screen mutants for defects in Spc42p–GFP assembly into the SPB, individual mutant strains were grown overnight at 23°C in media containing raffinose to mid-log phase and were shifted to 34°C for 30 min before a 70-min induction of *SPC42–GFP* expression by addition of galactose. Assembly of Spc42p–GFP into the SPB was scored by microscopic examination of cells. Mutants in which <50% of the cells ($n$ = 200) contained one or two discrete GFP foci were rescreened, and 48 putative assembly mutants were isolated. Spc42p–GFP levels in each mutant were analyzed by Western blotting with anti-GFP antibodies. 22 mutants were shown to express Spc42p–GFP at near wild-type levels at 34°C but were consistently defective in assembly of the protein into SPBs. In 8 of the 21 recessive mutants defining seven complementation groups, the SPB assembly defect cosegregated with the ts phenotype. Complementation of the ts phenotype with a plasmid library was used to identify the genes mutated in our SPB assembly mutants (Table I). An example of the assembly defect seen in one of the mutants meeting the criteria of the screen is shown in Fig. 1 (No. 99/*mps3-1*).

## Cloning of MPS3

A plasmid containing five putative ORFs from chromosome X rescued the growth defect of mutant No. 99 (*mps3-1*)

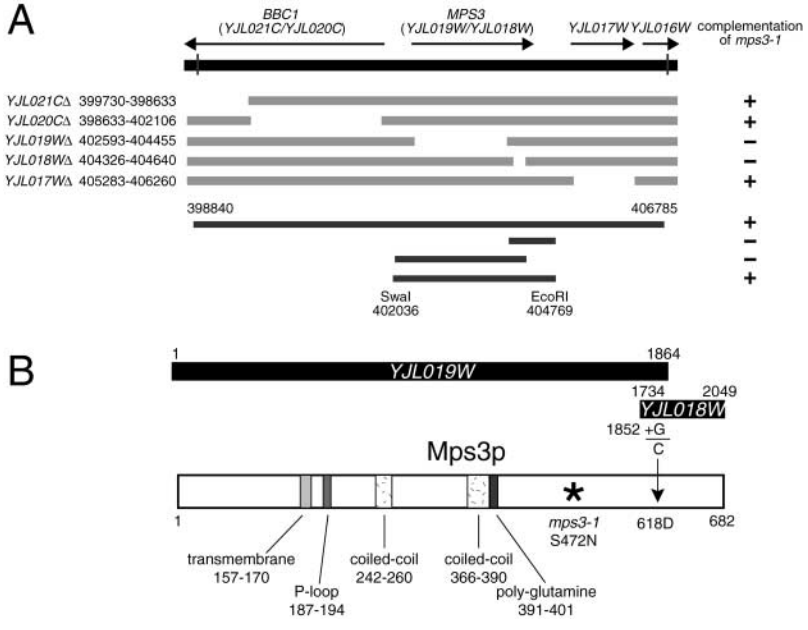


Figure 2. ***MPS3* encodes a 79-kD protein with several motifs.** (A) A single clone containing DNA from coordinates 398840 to 406785 on chromosome X was able to complement the temperature sensitivity of *mps3-1*. *mps3-1* mutants were crossed to deletion mutants of each ORF and tested for the ability to grow at 37°C. Diploids heterozygous for *mps3-1* and *YJL018WΔ* or *YJL019WΔ* were still ts for growth, whereas *YJL017WΔ*, *YJL020CΔ*, or *YJL021CΔ* were able to complement the growth defect of *mps3-1*. Subcloning various regions of the complementing plasmid and retesting for complementation of the ts phenotype revealed that both *YJL018W* and *YJL019W* were required to suppress the *mps3-1* growth defect. (B) Sequence analysis revealed that *YJL018W* and *YJL019W* correspond to a single gene encoding a 682–amino acid, 79-kD protein (Mps3p) due to an extra guanosine nucleotide at position 1852. ProDom, Pfam, and COILs programs were used to predict motifs in Mps3p: a transmembrane domain (light gray), a P-loop (gray), two coiled-coil domains (white/hatched), and a poly-glutamine track (black). *mps3-1* is caused by a G to A transition at nucleotide 1415, resulting in an asparagine (N) at amino acid 472.

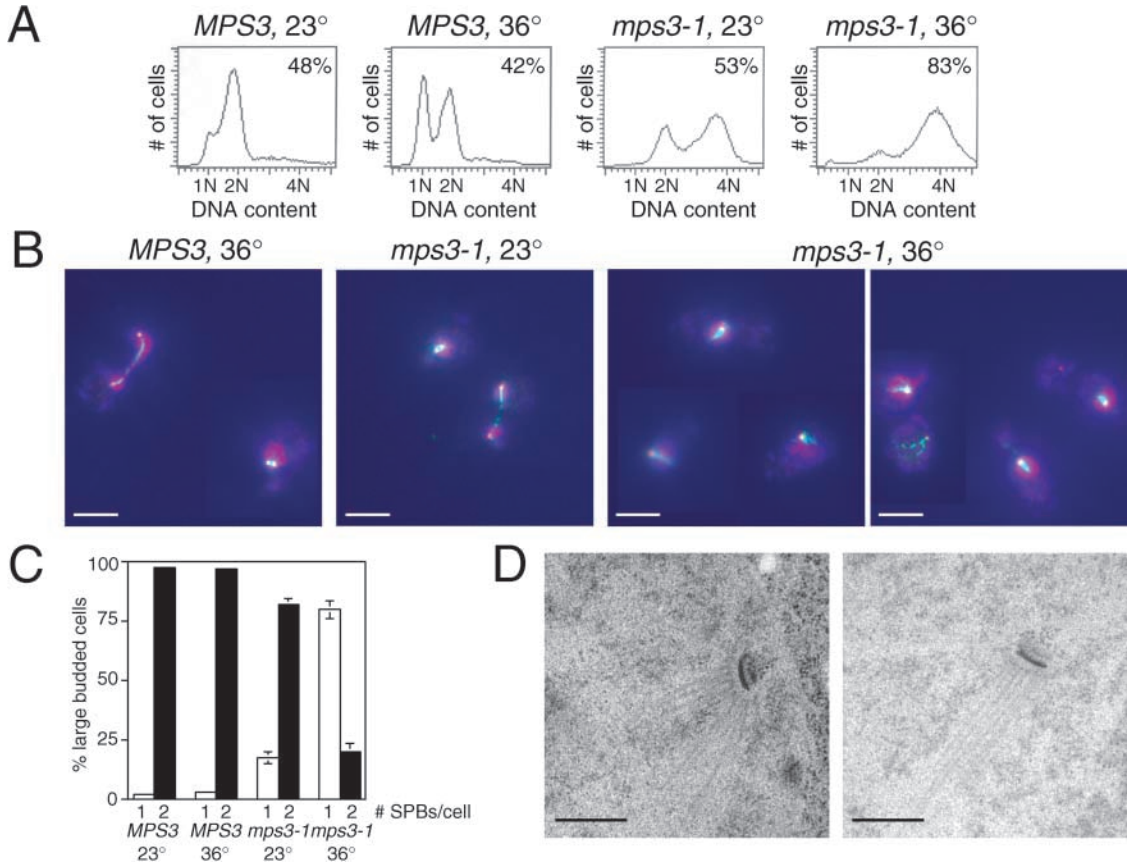


Figure 3. **Mps3p is required for SPB duplication.** Wild-type (SLJ001) and *mps3-1* mutant (SLJ910) cells were grown to mid-log phase at 23°C, cultures were divided, and half were shifted to 36°C for 4 h. (A) Flow cytometric analysis of DNA content and quantitation of budding index indicated that *mps3-1* mutants arrest in mitosis at 36°C. The biphasic peaks in wild-type cells represent cells with G1 (1N) and G2/M (2N) DNA content. At 23°C, *mps3-1* mutants have diploid DNA content (2N and 4N) and arrest at 36°C with replicated DNA (4N). The percentage of large budded cells for each sample is indicated ($n = 200$). (B) Indirect immunofluorescence was also performed to visualize the microtubules (green), SPBs (anti-Tub4p, red), and DNA (DAPI, blue). At 23°C, *mps3-1* mutants were able to form a bipolar mitotic spindle. However, at 36°C, *mps3-1* mutants arrested with a monopolar spindle and a single mass of DNA. Bars, 5 μm. (C) For each immunofluorescence sample, 200 large budded cells were examined, and the number of bipolar (black bars) versus monopolar (white bars) spindles determined by counting the number of Tub4p signals per cell. Percentages are averages based on three independent experiments. (D) To verify that *mps3-1* mutants contain a single SPB, 19 complete nuclei from large budded *mps3-1* mutants grown at 36°C were examined by EM. 14 nuclei contained a single SPB and a monopolar spindle (74%), and five nuclei contained two SPBs and a short bipolar spindle. A thin section image from two cells with a single SPB is shown. Bars, 0.4 μm.

(Fig. 2 A). Two of the ORFs were predicted to encode overlapping, essential genes (*YJL018W* and *YJL019W*), and diploids heterozygous for *mps3-1* and *YJL018WΔ* or *YJL019WΔ* were still ts for growth, suggesting that one or both of these genes is mutated in *mps3-1*. Neither ORF could rescue *mps3-1*, but a plasmid containing both ORFs was able to complement the *mps3-1* growth defect (Fig. 2 A). We sequenced the region of overlap between *YJL018W* and *YJL019W* from three different laboratory yeast strains, W303, S288c, and SK-1, and found an extra G/C base pair at position 1852 in *YJL019W* in all three strains (Fig. 2 B). This extra base pair results in a frame shift that joins *YJL018W* and *YJL019W* into a single, contiguous 2,049–base pair ORF. We sequenced the entire *YJL019W/YJL018W* gene from *mps3-1* and found a single G to A transition at nucleotide 1415, resulting in a change of serine 472 to an asparagine (Fig. 2 B). We conclude that *YJL019W/YJL018W* is a single gene that we call *MPS3* (monopolar spindle). The 682–amino acid protein encoded by *MPS3* has no clear homologues in other organisms but does contain several motifs found in other SPB proteins, including two predicted coiled-coil domains and a potential transmembrane domain (Fig. 2 B).

## Genetic phenotypes suggest that *MPS3* functions at the SPB

Because of the SPB assembly defect in *mps3-1*, we were interested in determining if *MPS3* is also required for SPB duplication. A second phenotype of *mps3-1* uncovered during backcrossing supported this possibility. Similar to some *cdc31* and *kar1* mutants, strains containing *mps3-1* diploidize immediately upon germination (Fig. 3 A) (Schild et al., 1981; Rose and Fink, 1987). Further evidence that Mps3p is linked functionally to the SPB is that many double mutants between *mps3-1* and SPB components are inviable, and most viable double mutants show enhanced growth defects at semi-permissive temperatures (Table II). Interestingly, *mps3-1* showed synthetic interactions with mutants in

Table II. ***mps3-1* genetically interacts with SPB components**

| Lethal | Sick | None |
|---|---|---|
| *cmd1-1* | *cdc31-2* | *tub4-1* |
| *mps1-8* | *kar1Δ-17* | |
| *mps2-1* | *mps1-1* | |
| *spc29-3* | *spc42-10* | |
| *spc110-220* | *spc42-11* | |
| *CDC31-16* | *spc98-2* | |

Heterozygous diploids were generated by crossing SJL910c to the indicated single haploid mutant strains. For each cross, 20–40 tetrads were dissected and analyzed. The *MPS3* plasmid was maintained during sporulation, and plasmid loss was assayed during tetrad analysis. "Lethal" indicates that no viable double mutant spores were obtained at 23°C. "Sick" indicates that the double mutant was inviable at a temperature permissive for growth for the single mutant parents. "None" indicates that the double mutant was equally competent for growth.

all steps of SPB duplication and with proteins located in different structures in the SPB.

## *mps3-1* mutants form monopolar spindles due to a SPB duplication defect

To determine if the *mps3-1* mutant shows defects in SPB duplication, asynchronously growing wild-type and *mps3-1* strains were analyzed after a 4-h shift to the nonpermissive temperature (36°C). Flow cytometric analysis of DNA content and budding index confirmed that *mps3-1* mutants arrest in mitosis at 36°C (Fig. 3 A). We examined the spindle phenotype in these cells using indirect immunofluorescence microscopy. At the nonpermissive temperature, 80% of large budded *mps3-1* cells have a monopolar spindle: a single microtubule aster nucleated by a single SPB and one mass of DNA (Fig. 3, B and C). In contrast, only 17% of large budded *mps3-1* cells grown at the permissive temperature contained monopolar spindles, and the remaining 83% contained bipolar spindles. Bipolar spindles were observed in 97% of large budded wild-type cells grown at 23°C or 36°C.

At the permissive temperature, the spindle structure of *mps3-1* mutants differs from that observed in wild-type cells in two aspects. First, the significant number of monopolar spindles seen in the mutant suggests that *mps3-1* is compromised for function at the permissive temperature (Fig. 3 C), likely contributing to the increase in ploidy phenotype in *mps3-1* strains. Second, 73% of the mitotic spindles in *mps3-1* mutants grown at 23°C are short metaphase spindles, which we rarely observe in wild-type cells (17%; unpublished data). As a result, we frequently observe a mitotic delay in *mps3-1* cells grown under permissive conditions.

Serial thin sections of entire nuclei from 19 large budded *mps3-1* cells grown at 36°C were examined by EM to verify that cells contain a monopolar spindle. Consistent with immunofluorescence analysis, 14 of 19 nuclei (74%) contained a single SPB and a monopolar spindle (Fig. 3 D). The SPB structure observed in *mps3-1* mutants is similar to that in *cdc31* and *kar1* mutants (Byers, 1981; Rose and Fink, 1987): the core SPB is intact, but the half-bridge is small and indistinct, and no satellite structure could be detected. Based on these observations, we conclude that *MPS3* is required for SPB duplication.

## MPS3 is required early in G1 for SPB duplication

The absence of a distinguishable half-bridge in *mps3-1* suggests that Mps3p, like Cdc31p and Kar1p, is needed for the earliest step of SPB duplication. We performed an execution point experiment to determine which stage of SPB duplication requires *MPS3* function. Wild-type and *mps3-1* cells

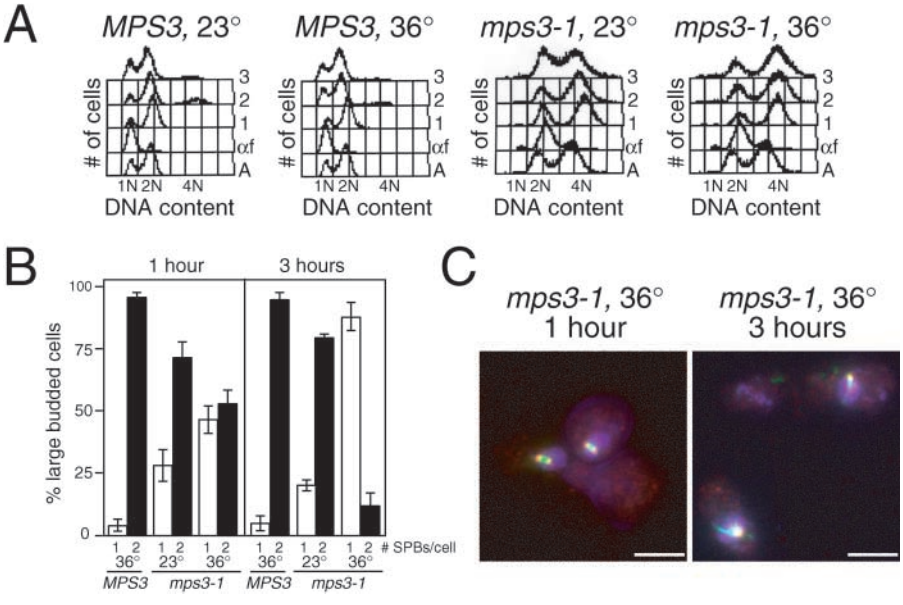


Figure 4. **Mps3p is required early in G1 for SPB duplication.** Wild-type (SLJ001) and *mps3-1* mutant (SLJ910) cells were synchronized in G1 by treatment with 1 μg/ml α-factor for 4 h at 23°C and then released into fresh media at 23°C or 36°C. Samples from each culture 1, 2, and 3 h after release from α-factor (αf) were removed and analyzed. Asynchronous cells (A) are shown as controls. (A) Flow cytometric analysis of DNA content indicated that *mps3-1* mutants at 36°C do not arrest during the first mitosis. The biphasic peaks in wild-type cells represent cells with G1 (1N) and G2/M (2N) DNA content. *mps3-1* mutants in G1 and G2/M have a 2N and 4N DNA content, respectively. (B) For each sample, cells were examined by indirect immunofluorescence microscopy. At 1 and 3 h after release, the number of bipolar (black bars) and monopolar (white bars) spindles was determined by counting the number of Tub4p signals per cell ($n$ = 200). Numbers are averages based on three independent experiments. (C) Indirect immunofluorescence images from *mps3-1* mutants released for 1 and 3 h from α-factor at 36°C show that Mps3p function is not required for SPB duplication and bipolar spindle formation during the first mitosis, but that Mps3p is required for SPB duplication and bipolar spindle formation during the second cell cycle. The mitotic spindle was detected using anti-tubulin antibodies (green), SPBs were visualized with anti-Tub4p antibodies (red), and DNA was stained with DAPI (blue). Bars, 5 μm.

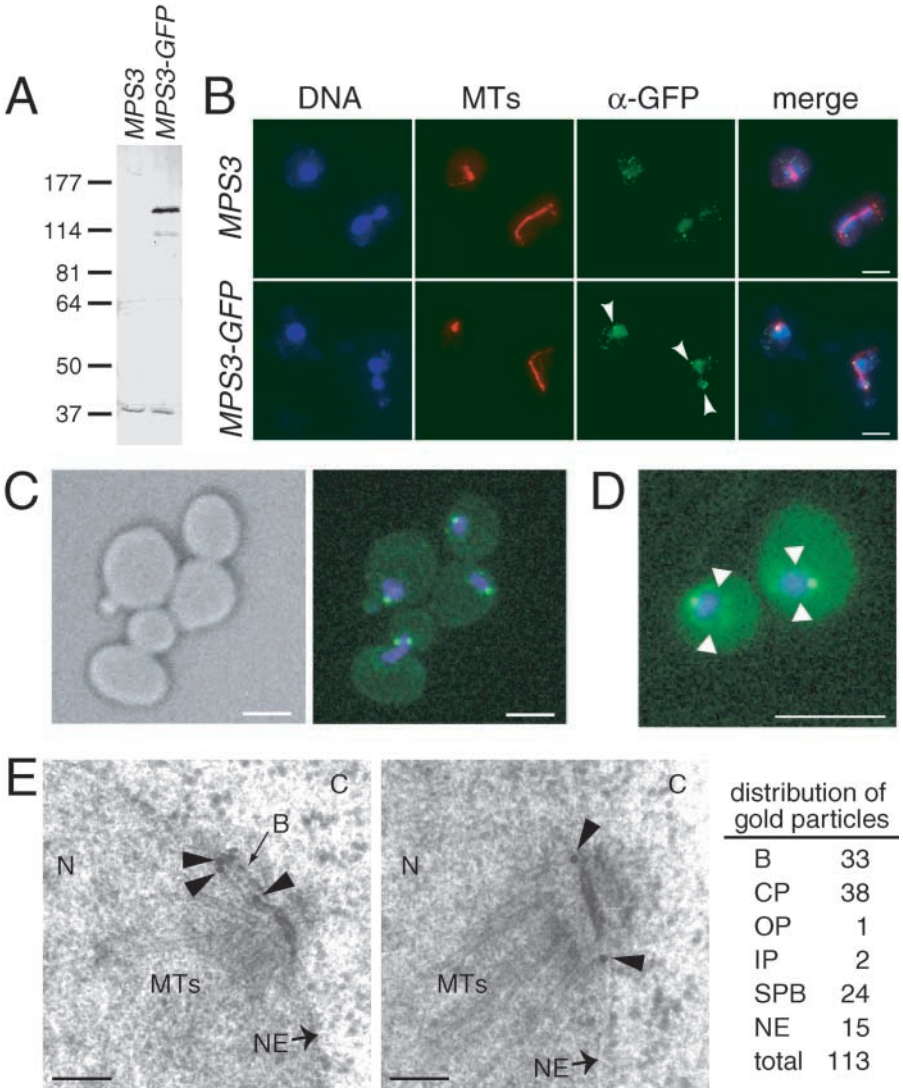


Figure 5. **Mps3p is a component of the SPB.** Wild-type diploid cells (SLJ126) and homozygous diploids containing *MPS3–GFP* (SLJ915) were grown to mid-log phase at 23°C. (A) Cells were harvested, and lysates were analyzed by Western blotting with anti-GFP antibodies. (B) Paraformaldehyde-fixed wild-type and Mps3p–GFP cells were stained with DAPI to visualize the DNA (blue), anti-tubulin antibodies to recognize microtubules (red), and anti-GFP antibodies to localize Mps3p–GFP (green, arrows). The merged image shows that Mps3p–GFP localizes to discrete foci at the poles of the mitotic spindle (yellow). Bar, 5 μm. (C and D) Mps3p–GFP localization was also analyzed in living cells by epifluorescence microscopy. Mps3p–GFP (green) appears as one to two foci coincident with the DNA (blue). In addition, a fraction of Mps3p–GFP was also detected at the nuclear envelope (D, arrows). Bar, 5 μm. (E) Localization of Mps3p–GFP to the SPB was confirmed by immuno-EM using anti-GFP antibodies and colloidal gold–conjugated secondary antibodies. Thin sections of two different cells are shown. The SPB is embedded in the nuclear envelope (NE), which separates the nucleus (N) and cytoplasm (C). Microtubules (MTs) can be see on the nuclear side of the SPB. Arrowheads indicate the position of the gold particles that recognize Mps3p–GFP. A total of 37 SPBs were analyzed, and the distribution of gold particles to the central plaque (CP), outer plaque (OP), inner plaque (IP), bridge (B), and nuclear envelope (NE) is indicated. In some sections, localization to a discrete SPB substructure could not be determined (SPB). Bar, 0.1 μm.

were arrested at an intermediate step of SPB duplication at 23°C using α-factor (the satellite has formed at the distal end of the half-bridge but further SPB assembly is inhibited) and then were released into fresh media at 23°C or 36°C. 1 h after release from α-factor arrest, the majority of cells had entered the first mitosis, as judged by bud formation and DNA replication (Fig. 4 A). Virtually all large budded wild-type cells examined at this time point contained bipolar mitotic spindles (Fig. 4 B). Although monopolar spindles were seen in *mps3-1* mutants grown at 23°C or 36°C, greater than 50% of large budded *mps3-1* mutants were able to form a bipolar mitotic spindle during the first mitosis (Fig. 4, B and C), indicating that *MPS3* function is not required for later steps of SPB duplication. Instead, *mps3-1* mutants appear to fail in SPB duplication during the second cell cycle. At 3 h after α-factor release, 88% of large budded *mps3-1* cells grown at 36°C now contained a monopolar spindle (Fig. 4, B and C).

The ability of *mps3-1* to complete SPB duplication at 36°C after release from α-factor is unlikely the result of incomplete inactivation of mps3-1p because preincubation of cells at 36°C for 1 h immediately before α-factor release gave virtually identical results (unpublished data). Furthermore, *mps3-1* is capable of a first cycle arrest. Cells released from S-phase (hydroxyurea) arrest in mitosis with monopolar spindles after undergoing a single failed round of SPB duplication in the absence of Mps3p function (unpublished data). These data indicate that *MPS3* is required before the satellite-bearing stage of SPB duplication, although we cannot exclude the possibility that other alleles will show requirements for *MPS3* in additional steps.

### Mps3p localizes to the SPB half-bridge

To understand its role in SPB duplication, we examined the Mps3p protein. *MPS3* is predicted to encode a 79-kD protein. To verify this prediction and demonstrate that *YJL018W* and *YJL019W* are one gene, we constructed a yeast strain in which the endogenous copy of *MPS3* is fused at its COOH terminus to GFP (*MPS3–GFP*). Cells expressing Mps3p–GFP, but not an untagged control, contained a single protein of ~120 kD that was recognized by anti-GFP antibodies (Fig. 5 A). Because GFP is 27 kD, this indicates that Mps3p migrates as a 90–95-kD protein on our gel system.

Analysis of Mps3p–GFP localization in living and fixed cells showed that Mps3p is an SPB component. In cells fixed

for indirect immunofluorescence microscopy, we observed one or two discrete, bright foci of Mps3p–GFP staining coincident with the ends of the microtubules present only in the strain containing the GFP fusion (Fig. 5 B), consistent with localization to the SPB. Similar to the pattern we observed in fixed cells, one or two bright spots of GFP autofluorescence were seen at the periphery of the nuclear DNA in living cells (Fig. 5 C). In addition, we also detected faint Mps3p–GFP fluorescence around the DNA in live cells (Fig. 5 D), suggesting that Mps3p may reside at the nuclear envelope in addition to the SPB. Localization of Mps3p–GFP to the SPB does not appear to change during cell division, as we observed the protein at the SPB in cells at all cell cycle stages (Fig. 5, B and C).

We performed immuno-EM on asynchronously growing *MPS3–GFP* cells to further refine the subcellular localization of Mps3p. We were able to detect Mps3p–GFP at 37 of 40 SPBs examined using anti-GFP antibodies (Fig. 5 E). Within the SPB, we rarely detected gold particles at the inner plaque (IP) or outer plaque (OP) regions of the SPB. Like the examples shown in Fig. 5 E, virtually all the gold particles at the SPB (96%) were found at the half-bridge (B) or at the interface between the half-bridge and central plaque (CP), suggesting that Mps3p is a component of the SPB half-bridge. These gold particles were most frequently observed on the nuclear side of the half-bridge (Fig. 5 E), however, some were clearly on its cytoplasmic face (unpublished data). We also observed that a fraction of the gold particles (13%) was distributed randomly in the nuclear envelope (NE), not at the SPB, consistent with observations in living cells of an additional perinuclear localization for Mps3p–GFP (Fig. 5, C and D).

## Mps3p is an integral membrane protein

Our immuno-EM analysis suggests that Mps3p is a half-bridge protein. Because Mps3p contains a putative transmembrane domain, we might expect that it is a membrane protein of the half-bridge like Kar1p (Vallen et al., 1992b). To determine if Mps3p associates with membranes, spheroplasts were prepared from cells containing a COOH-terminal fusion of *MPS3* to three copies of the HA epitope (*MPS3–HA3)*. After a mild lysis, extracts were fractionated by differential centrifugation, and the distribution of Mps3p–HA3 to the supernatant and pellet fractions was determined by Western blotting. Mps3p–HA3 was detected almost exclusively in the pellet fraction (P) that contains the cellular membranes (Fig. 6). The cytoplasmic protein Zwf1p was a minor contaminant in our membrane preparations, whereas the membrane protein Vam3p was greatly enriched in the pellet fraction (Fig. 6) (Srivastava and Jones, 1998; Kumar et al., 2002). The fact that Mps3p–HA3 could only be extracted from the pellet in the presence of the detergent Triton X-100 indicates that Mps3p, like Vam3p, is an integral membrane protein (Fig. 6).

## Mps3p interacts with Cdc31p

We were interested in determining the binding partner(s) of Mps3p within the organelle to better understand its role in SPB duplication. Two obvious candidates were Cdc31p and Kar1p. We were unable to coimmunoprecipitate either Cdc31p or Kar1p with Mps3p, however, as previously reported (Spang et al., 1995), and we were also unable to coimmunoprecipitate Cdc31p with Kar1p (unpublished data). Therefore, to ask if Mps3p could bind to Cdc31p, we used a gel overlay assay. Full-length Kar1p and amino acids 171–682 of Mps3p (Mps3p-Ct) expressed as GST fusion proteins in bacteria were transferred to nitrocellulose after SDS-PAGE of bacterial extracts, and the membrane was probed with recombinant Cdc31p labeled with the infrared dye Alexa®680. Cdc31p bound to GST–Kar1p and GST–Mps3p-Ct, but it did not interact with GST or with other proteins in the bacterial extracts (Fig. 7 A). Binding of Cdc31p to Mps3p in the gel overlay assay was weak, but reproducible, and occurred in the presence of calcium or EGTA (unpublished data).

If Mps3p and Cdc31p interact in vivo, we might expect that mutations in *MPS3* would exacerbate the growth defect of *cdc31* mutants. Analysis of *mps3-1 cdc31-2* and *mps3-1 CDC31-16* strains revealed that the double mutants showed slow growth and reduced viability at permissive temperatures when compared with the single mutant strains (Fig. 7 B). Additional evidence that Cdc31p and Mps3p associate in vivo comes from the observation that overexpression of *CDC31* suppressed the growth defect of *mps3-1* mutants at 36°C (Fig. 7 C). Overexpression of other SPB genes, including *KAR1*, was unable to restore growth to *mps3-1* (unpublished data). These results suggest that Mps3p interacts with Cdc31p in yeast.

We examined the localization of Cdc31p in *mps3-1* to determine if Mps3p is involved in its recruitment to the SPB. Using affinity-purified anti-Cdc31p antibodies, we were able to detect Cdc31p at SPBs in nearly all wild-type cells examined (Fig. 7 D). Cdc31p was also found at SPBs in

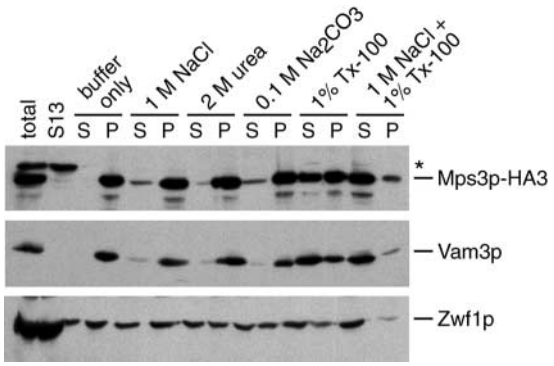


Figure 6. **Mps3p is an integral membrane protein.** Spheroplasts were prepared from cells expressing Mps3–HA3 from the endogenous promoter (SLJ922). A total cellular extract (total) from the spheroplasts was centrifuged at 13,000 *g* to separate membrane-associated (pellet, P) and soluble proteins (S13). The membrane fraction was resuspended in lysis buffer and extracted with 1 M NaCl, 2 M urea, 0.1 M $Na_2CO_3$, pH 11, 1% Triton X-100, or 1% Triton X-100 and 1 M NaCl or mock extracted (buffer). After a 15-min incubation on ice, samples were recentrifuged at 13,000 *g* to generate supernatant (S) and pellet (P) fractions. Immunoblotting indicates that Mps3p–HA3 fractionates with the integral membrane protein Vam3p and not with the cytoplasmic protein Zwf1p. The asterisk indicates a nonspecific background band recognized by the anti-HA antibody.

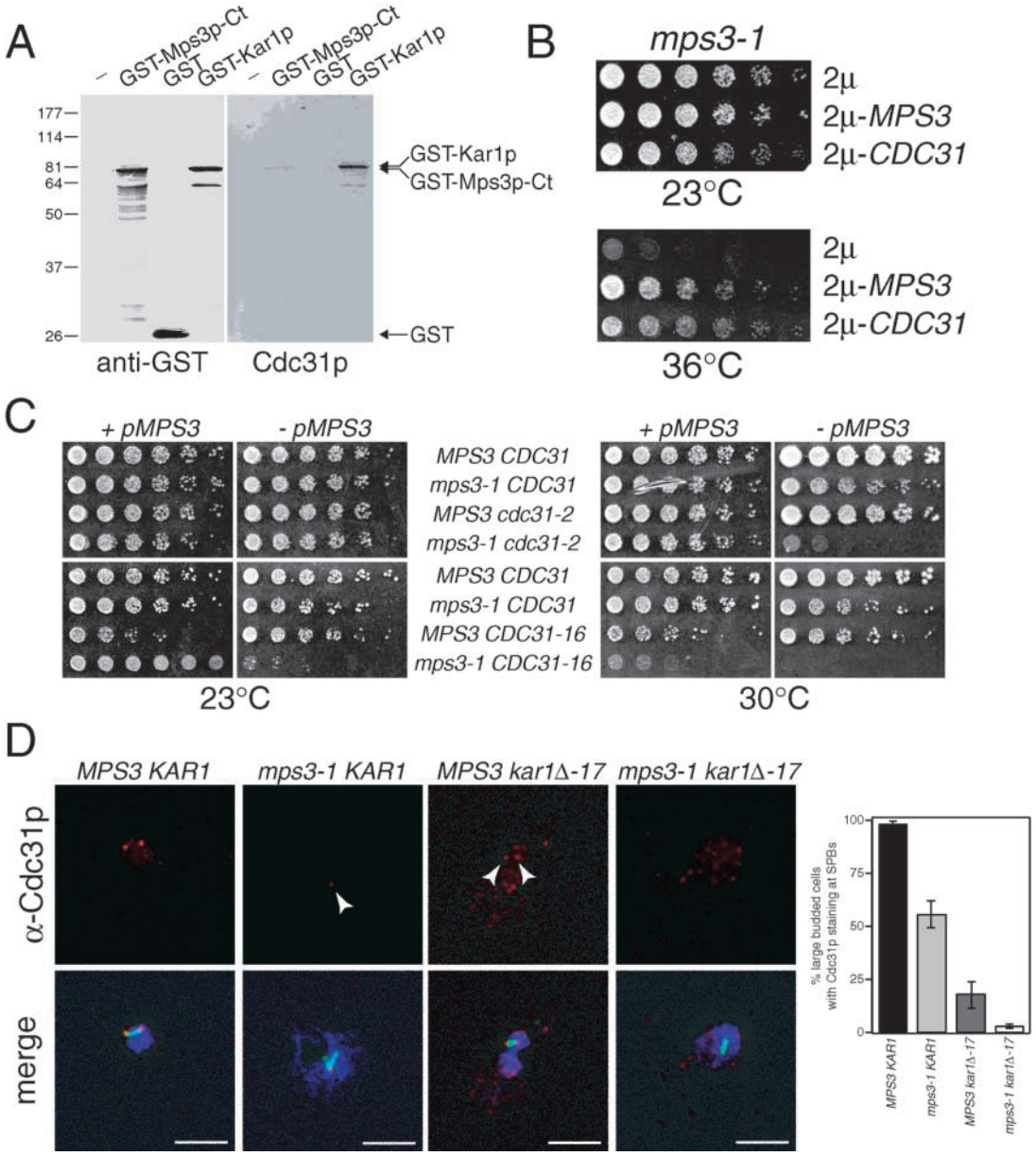


Figure 7. **Mps3p interacts with Cdc31p.** (A) Bacterial extracts from cells expressing GST, GST–Kar1p, GST–Mps3p-Ct, or nothing (−) were electrophoretically separated, and proteins were transferred to nitrocellulose. Expression of GST and the GST fusion proteins was detected by Western blotting with anti-GST antibodies (left). Membranes were also probed with purified 6His–Cdc31p labeled with the infrared dye Alexa®680 in a gel overlay assay to determine if proteins in each extract were capable of binding Cdc31p (right). (B) 2μ plasmids containing *MPS3* or *CDC31* or the empty vector were transformed into *mps3-1* (SLJ910). Cells were grown in media lacking uracil overnight at 23°C to a density of ~4 $OD_{600}$ U/ml, serially diluted fourfold, and spotted onto SD URA$^-$ plates. Plates were incubated at 23°C or 36°C for 3 d. (C) The *mps3-1* mutant (SLJ775) was crossed to strains containing mutations in *CDC31* (*cdc31-2*, SLJ809, and *CDC31-16*, SLJ906). After loss of plasmids in the heterozygous diploid, p*URA3-MPS3* (pSJ140) was retransformed, and cells were sporulated at 23°C, dissected, and analyzed. Progeny from tetratype spores were grown overnight at 23°C to a density of ~5 $OD_{600}$ U/ml, serially diluted fourfold, and spotted onto SD URA$^-$ or 5-fluoro-orotic acid plates. Plates were incubated for 3 d at 23°C or 30°C. (D) The *mps3-1* mutant (SLJ775) was crossed to the *kar1-Δ17* mutant (SLJ843), and localization of Cdc31p in progeny from a tetratype tetrad was analyzed after a 4-h shift to 36°C. Cells were stained with anti-Cdc31p (red) and anti-tubulin (green) antibodies and with DAPI (blue) to visualize DNA. Arrows point to the diminished Cdc31p signal in *mps3-1* and *kar1-Δ17*. No Cdc31p staining was observed in *mps3-1 kar1-Δ17*. The graph summarizes three independent localization experiments using two independently derived tetrads ($n$ = 200 in each sample). Bars, 5 μm.

*mps3-1* cells grown at 23°C (unpublished data). However, when *mps3-1* mutants were shifted to the nonpermissive temperature (36°C), Cdc31p staining at the SPBs was diminished and was visible in only 54% of cells (Fig. 7 D), suggesting that Mps3p is required for efficient recruitment of Cdc31p to SPBs. For comparison, we also examined Cdc31p localization in cells containing a mutation in the other Cdc31p binding partner, Kar1p. In contrast to previous studies (Biggins and Rose, 1994; Spang et al., 1995), we were able to detect Cdc31p at the SPB in 17% of *kar1-Δ17* mutants grown at 36°C (Fig. 7 D). We suspect that superior detection using a digital camera allowed us to detect Cdc31p

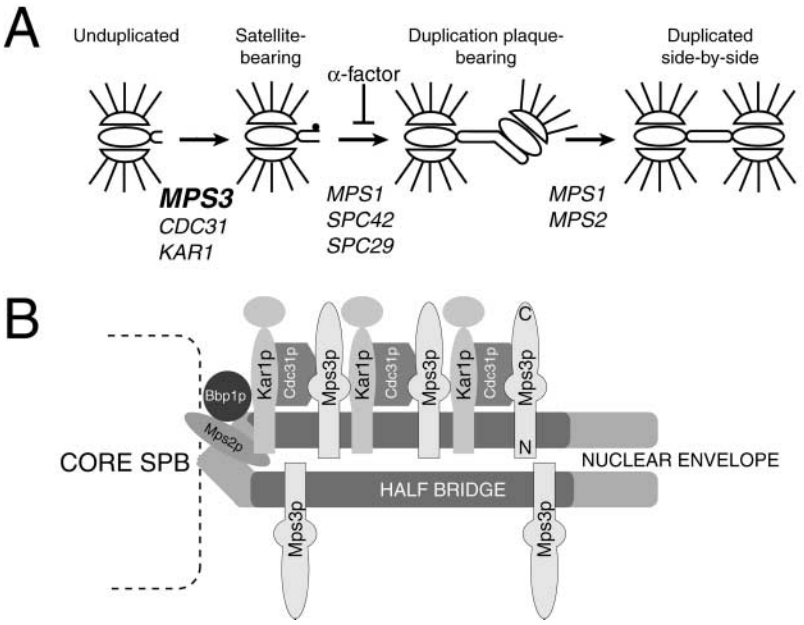


Figure 8. **Model for the role of Mps3p in the SPB duplication pathway.** (A) Based on previous studies of loss of function mutant alleles, the requirements of the various gene products that we discuss in this study in the SPB duplication pathway can be inferred (for reviews see Chial and Winey, 1999; Adams and Kilmartin, 2000). Our data suggest that Mps3p is required for the early step of SPB duplication (see Discussion). However, we cannot exclude the possibility that Mps3p, like other SPB assembly factors such as Mps1p, functions at additional steps in SPB duplication. (B) Based on the interaction between the COOH terminus of Mps3p and Cdc31p, we predict that the $NH_2$ terminus of Mps3p anchors the protein in the membrane and the COOH terminus is exposed to the cytoplasm and nucleoplasm. Cdc31p localizes to the cytoplasmic face of the SPB (Spang et al., 1993), suggesting that Mps3p is also here. However, our immuno-EM analysis indicates that at least some fraction of Mps3p might be on the nuclear side of the envelope as well.

at the SPB in *kar1* mutants, especially because the Cdc31p signal in *mps3-1* and *kar1-Δ17* mutants was often reduced compared with wild type (Fig. 7 D). The fact that we were unable to detect Cdc31p at the SPB in *mps3-1 kar1-Δ17* (Fig. 7 D) indicates that residual Cdc31p at the SPB in *mps3-1* is due to Kar1p and suggests that Mps3p and Kar1p are the two Cdc31p binding partners at the SPB.

## Discussion

We conclude that Mps3p is a novel component of the SPB half-bridge. The remarkably similar terminal phenotypes observed in *mps3*, *kar1*, and *cdc31* mutants and the requirement for *MPS3* and *CDC31* before the α-factor arrest point strongly suggest that Mps3p functions at the same step in SPB duplication as Cdc31p and Kar1p (Byers, 1981; Rose and Fink, 1987; Winey et al., 1991). All three proteins are essential for half-bridge elongation and satellite formation in wild-type yeast cells (Fig. 8 A). We have shown that Mps3p not only localizes to the SPB half-bridge, but also associates with Cdc31p. Binding between Cdc31p and the COOH terminus of Mps3p suggests a specific function for Mps3p in SPB duplication, and it allows us to predict the topology of Mps3p in the nuclear membrane (Fig. 8 B).

*MPS3* is an essential gene, and our observations that *mps3-1* mutants arrest with monopolar spindles at the nonpermissive temperature are consistent with the possibility that its essential function is in SPB duplication. However, this does not exclude other Mps3p functions. The *mps3-1* mutant exhibits several phenotypes at the permissive temperature, including a delay in metaphase. Although a partial SPB defect at the permissive temperature could explain the mitotic delay, the fact that it is not alleviated by deletion of spindle checkpoint genes (*MAD1*, *MAD2*, or *MAD3*; unpublished data) suggests that *mps3-1* is defective in a second process. Localization of a fraction of Mps3p to the nuclear periphery suggests that Mps3p could be involved in some aspect of nuclear membrane function. Cdc31p and Kar1p have multiple functions in the cell (Vallen et al., 1992a; Sullivan et al., 1998), and Mps3p might also participate in these processes.

*MPS3* encodes a novel SPB component, but *MPS3* shares features common to other genes encoding SPB proteins. First, the predicted protein has two potential coiled-coil domains between residues 242–260 and 366–390 (Wigge et al., 1998). Second, the promoter of *MPS3* contains two partial matches to the MluI cell cycle box (ACGCGTNA) at positions −209 to −202 (ACGgGTAA) and −193 to −186 (ACGCGaAA) (McIntosh et al., 1991). This promoter element leads to G1-specific gene transcription and is found in the promoters of *SPC110* and *SPC42* (Kilmartin et al., 1993; Donaldson and Kilmartin, 1996). mRNA levels of *MPS3* (both *YJL019W* and *YJL018W*) are highest in G1 (Spellman et al., 1998), suggesting that expression of Mps3p is cell cycle regulated.

*MPS3* was not found using other protein-based techniques used to analyze SPB composition. Two-hybrid analysis, including a *CDC31* two-hybrid screen, has been used extensively to analyze protein–protein interactions within the SPB and to identify new SPB components (Sullivan et al., 1998; Schramm et al., 2001). In addition, SPBs have been enriched from yeast and the protein composition of the SPB analyzed by mass spectrometry (Wigge et al., 1998). Mps3p was not detected by these methods. However, most also failed to identify the other membrane protein of the half-bridge, Kar1p.

In addition to Mps3p, Cdc31p also binds to Kar1p (Biggins and Rose, 1994; Spang et al., 1995). In fact, the essential function of Kar1p in SPB duplication is to recruit Cdc31p to the SPB. Kar1p is thought to be the primary binding partner for Cdc31p at the SPB, but a second Cdc31p binding partner had been postulated (Vallen et al., 1994). The most compelling evidence for a second Cdc31p binding partner comes from observations that a dominant allele of *CDC31*, *CDC31-16*, suppresses a complete deletion of *KAR1* and that the protein encoded by this mutant,

Table III. **Yeast strains**

| Strain | Relevant genotype |
|---|---|
| SLJ001 | *MATa bar1* |
| SLJ126 | *MATa/MATα* |
| SLJ761 | *MATa ura3::GAL-SPC42-GFP-URA3* |
| SLJ753 | *MATa mps1-1 ura3::GAL-SPC42-GFP-URA3* |
| SLJ756 | *MATa spc29-3 ura3::GAL-SPC42-GFP-URA3* |
| SLJ859 | *MATa/MATa mps3-1/mps3-1 ura3::GAL-SPC42-GFP-URA3/ura3::GAL-SPC42-GFP-URA3* |
| SLJ764 | *MATa ura3::GAL-SPC42-GFP-URA3 his3::GAL-H2B1-LACZ-HIS3* |
| SLJ910 | *MATa/MATa bar1/bar1 mps3-1/mps3-1* |
| SLJ910c | *MATa bar1 mps3-1 pURA3-MPS3 (pSJ140)* |
| SLJ915 | *MATa/MATα MPS3::MPS3-GFP-KANMX6/MPS3::MPS3-GFP-KANMX6* |
| SLJ922 | *MATa MPS3::MPS3-HA3-HIS3MX6* |
| SLJ809 | *MATa cdc31-2 pURA3-CDC31* |
| SLJ906 | *MATa CDC31-16 pURA3-CDC31* |
| SLJ843 | *MATa kar1-Δ17 pURA3-KAR1* |

All strains were generated as part of this study.

Cdc31-16p, localizes to the SPB in the complete absence of Kar1p (Biggins and Rose, 1994). Our findings that a *mps3-1 CDC31-16* strain is unable to grow at any temperature, that overexpression of wild-type *CDC31* rescues the growth defect of *mps3-1*, and that Cdc31p binds Mps3p in vitro suggest that Mps3p might be the other protein that binds Cdc31p at the half-bridge. We confirmed this possibility by examining the localization of Cdc31p in *mps3-1* mutants. The fact that Cdc31p localization to the SPB is reduced in *mps3-1* or *kar1-Δ17* strains at 36°C and is abolished in the *mps3-1 kar1-Δ17* double mutant indicates that Kar1p and Mps3p are the half-bridge proteins required to recruit Cdc31p to the SPB (Fig. 8 B).

So how are Cdc31p, Kar1p, and Mps3p arranged at the half-bridge? We detect binding between Mps3p and Cdc31p, and genetic experiments also support the idea that Mps3p and Cdc31p interact. The weak signal seen in the Cdc31p gel overlay with Mps3p could arise from any number of reasons, including the use of a truncated form of Mps3p (full-length Mps3p did not express in bacteria; unpublished data), the use of unmodified, recombinant Cdc31p and Mps3p, inherent low affinity between Cdc31p and Mps3p, or the fact that Mps3p is denatured in this assay. Preliminary results from fluorescence resonance energy transfer experiments between Mps3p and other SPB components suggest that Mps3p and Kar1p interact in vivo (Muller, E., and T. Davis, personal communication). Perhaps Mps3p forms a trimeric complex with Cdc31p and Kar1p in vivo, and its primary function is to regulate the Kar1p–Cdc31p interaction rather than directly bind Cdc31p. The Cdc31p binding site in Kar1p has been identified by Kar1p deletion analysis and is a 19–amino acid acidic α-helix in the central part of Kar1p (Spang et al., 1995). We have yet to conclusively identify a similar site in the primary sequence of Mps3p, but Mps3p is predicted to contain multiple α-helical domains. Mps3p also contains several other protein–protein interaction domains that might mediate the formation of a complex with Cdc31p and Kar1p.

Mps3p, Kar1p, and Cdc31p all localize to the SPB throughout the cell cycle (Spang et al., 1993, 1995; Biggins and Rose, 1994), and we speculate that these are the structural proteins of the half-bridge. This raises an interesting question of how initiation of satellite formation is restricted to only once during early G1, given that the key half-bridge components are present at the SPB during the entire cell cycle. Although an exact equivalent of the half-bridge is not found in higher eukaryotic centrosomes, it does seem that an analogous template structure exists and is important for centrosome duplication (Adams and Kilmartin, 2000; Hinchcliffe and Sluder, 2001). Centrosomes are composed of two orthogonally oriented centrioles. During centrosome duplication, the centrioles split apart and a new centriole is built adjacent to the two preexisting centrioles. Assembly of the centriole precursor, the procentriole, occurs at a set distance from the existing centriole just as assembly of the SPB precursor, the satellite, occurs at a set distance from the existing SPB. The length of the half-bridge is what seems to determine the SPB/satellite distance, and recruitment of Cdc31p to the half-bridge is likely a key step in SPB duplication. Similarly, a fraction of centrin localizes to the region between the new and the old centriole, and it appears to play some role in controlling centrosome duplication (Paoletti et al., 1996; Salisbury et al., 2002). Therefore, understanding the mechanisms that regulate Mps3p and Kar1p function and their interaction with Cdc31p is relevant not only to yeast SPB duplication but also to centrosome duplication in other eukaryotes.

## Materials and methods

### Yeast strains and plasmids

All strains are derivatives of W303 (*ade2-1 trp1-1 leu2-3,112 his3-11,15 ura3-1 can1-100*) and are listed in Table III. Standard techniques were used for DNA and yeast manipulations, including sporulation and mating of the diploidized *mps3-1* strain (Guthrie and Fink, 1991).

Galactose-inducible *SPC42–GFP* and *H2B1–LACZ* were constructed by subcloning from pIA29 (Adams and Kilmartin, 1999) and pFB-67c (Moreland et al., 1987) into versions of pRS306 and pRS303 (Sikorski and Hieter, 1989) containing *GAL1/10*, respectively, and they were integrated into yeast to generate SLJ764. A 2.7-kb SwaI–EcoRI DNA fragment containing the entire *MPS3* ORF (*YJL019W* and *YJL018W*) was cloned into pRS316 (Sikorski and Hieter, 1989) to generate p*URA3-MPS3* (pSJ140). In frame fusions between *MPS3* and GFP or HA3 immediately before the *MPS3* stop codon were created in SLJ126 by PCR-based methods (Longtine et al.,

1998). pRS202-*MPS3* contains an 8.8-kb fragment including *MPS3*, and pRS202-*CDC31* contains a 1.5-kb HindIII fragment including *CDC31*. The ORFs of *KAR1* or *CDC31*, or the COOH-terminal region of the *MPS3* ORF (amino acids 171–682), were amplified by PCR from genomic DNA and inserted into bacterial expression vectors (pGEX-3X [Amersham Biosciences] for *KAR1* and *MPS3* and pQE-10 [QIAGEN] for *CDC31*).

### SPB assembly screen

A ts bank of mutants was created by mutagenizing five pools of SLJ764 with ethylmethane sulfonate to 60–70% killing as previously described (Rose et al., 1990). Strains unable to induce protein expression from the *GAL* promoter were eliminated from the collection using a β-galactosidase assay to monitor induction of H2B1–LacZp (Rose et al., 1990). Approximately 150,000 mutagenized cells yielded 755 ts strains that were microscopically screened for SPB assembly defects as described in the text. The gene responsible for the SPB assembly defect in each mutant was identified by complementation of the ts phenotype using a centromere-based library (Rose and Fink, 1987), linkage analysis, and intragenic complementation testing (Table I; Fig. 2). Two mutants were not cloned.

### Lysate preparation and Western blotting

Yeast lysates were prepared by resuspending 2 $OD_{600}$ U/ml of cells in 0.2 ml SDS sample buffer (125 mM Tris-HCl, pH 6.8, 5% SDS, 1.4 M β-mercaptoethanol, 20% glycerol, 0.3% bromophenol blue, 2 mM PMSF) and lysing by mechanical disruption. Proteins were fractionated by differential centrifugation as previously described (Srivastava and Jones, 1998). Samples equal to 0.5 $OD_{600}$ U/ml of cells were loaded on SDS-PAGE gels, and proteins were detected by immunoblotting with the following dilutions of antibodies: 1:2,000 anti-GFP mAb B34 (Covance); 1:1,000 anti-HA mAb 16B12 (Covance); 1:1,000 affinity-purified anti-Vam3p antibody (a gift of G. Odorizzi, University of Colorado); 1:20,000 affinity-purified glucose-6-phosphate dehydrogenase antibody (Zwf1p; Sigma-Aldrich).

### Cdc31p antibodies

Antibodies against purified 6His–Cdc31p (see below) were generated in rabbits (Animal Pharm) and purified according to the manufacturer's instructions on a Cdc31p column created using the Sulfo-link kit (Pierce Chemical Co.). Purified antibodies recognize a single major band the size of Cdc31p in yeast extracts (not depicted).

### Cytological techniques

The DNA content of 20,000 mid-log phase cells stained with propidium iodide was determined by flow cytometry as previously described (Hunter and Eipel, 1979). Samples were analyzed on a Becton Dickinson FACScan® flow cytometer using CELL QUEST software. Cells were fixed with 4% paraformaldehyde in 0.1 M sucrose for 20 min at room temperature, spheroplasted, methanol/acetone fixed to glass sides, and processed for immunofluorescence as previously described (Rose et al., 1990). The following primary antibody dilutions were used: microtubules, 1:500 rat anti-tubulin antibody YOL 1/34 (Accurate Chemical & Scientific Corp.); SPBs, 1:500 affinity-purified anti-Tub4p antibodies (a gift of T. Stearns, Stanford University, Palo Alto, CA); Mps3–GFP, 1:5,000 affinity-purified anti-GFP polyclonal antibodies (CLONTECH Laboratories, Inc.); and Cdc31p, 1:500 affinity-purified anti-Cdc31p antibodies. Secondary antibodies included 1:10,000 CY3-conjugated goat anti–rabbit IgG (Chemicon) and 1:200 fluorescein-conjugated goat anti–rat IgG (Cappel). DNA was visualized by staining with 1 μg/ml DAPI for 5 min immediately before mounting with Citifluor (Ted Pella, Inc.). Cells were examined with a Leica fluorescence microscope using 63× magnification, and images were captured with a Cooke Sensicam and processed with Slidebook (3I). Cells were high pressure frozen, freeze substituted, sectioned, and stained as previously described (Giddings et al., 2001) to examine spindle structure by EM or to detect Mps3p–GFP by immuno-EM. Serial thin sections were viewed on a Philips CM10 electron microscope, and images were captured with a Gatan digital camera and viewed with Digital Micrograph Software.

### Gel overlay assay

6His–Cdc31p was purified from M15 *Escherichia coli* transformed with pQE10-*CDC31* and induced with 0.5 mM IPTG for 2 h at 25°C by metal affinity chromatography using Talon resin as described by the manufacturer (CLONTECH Laboratories, Inc.). 500 μg of purified Cdc31p was dialyzed overnight at 4°C against PBS and labeled with the infrared dye Alexa®680 according to the manufacturer's instructions (Molecular Probes).

Expression of GST, GST–Kar1p, and GST–Mps3p-Ct in the *E. coli* strain BL21(DE3) was induced by the addition of 0.5 mM IPTG to log-phase cells for 2 h at 25°C. 10 μl of GST–Kar1p, GST–Mps3p-Ct, and cell only and 2 μl of GST extract from 1 ml culture were separated by 10% SDS-PAGE, and proteins were electrophoretically transferred to nitrocellulose membranes (Scheiler & Schuell). Membranes were probed with ~10 μg labeled 6His–Cdc31 as previously described (Biggins and Rose, 1994) and were imaged on an infrared scanner (LiCor) to detect Alexa®680–Cdc31p binding. Expression of bacterial fusion proteins was confirmed by Western blotting with a 1:1,000 dilution of anti-GST antibody (Amersham Biosciences).

We are grateful to T. Davis and E. Muller for discussions and sharing unpublished results. We thank S. Biggins, J. Kilmartin, T. Stearns, T. Davis, C. Boone, F. Winston, A. Bender, E. Steinmetz, G. Odorizzi, and S. vanKreefeld for reagents, J. Meehl, G. Morgan, P. Straight and H. Fisk for help with microscopy, S. Biggins, P. Straight, H. Fisk, A. Stemm-Wolf, and S. Jones for comments on the manuscript, and all the members of the Winey lab for valuable discussions and encouragement.

This work was supported by funding from the National Institutes of Health (GM51312 to M. Winey), the Keck Foundation (to S.L. Jaspersen), and the Helen Hay Whitney Foundation (to S.L. Jaspersen).

Submitted: 28 August 2002
Revised: 6 November 2002
Accepted: 6 November 2002

## References

Adams, I.R., and J.V. Kilmartin. 1999. Localization of core spindle pole body (SPB) components during SPB duplication in *Saccharomyces cerevisiae*. *J. Cell Biol.* 145:809–823.

Adams, I.R., and J.V. Kilmartin. 2000. Spindle pole body duplication: a model for centrosome duplication. *Trends Cell Biol.* 10:329–335.

Ball, C.A., K. Dolinski, S.S. Dwight, M.A. Harris, L. Issel-Tarver, A. Kasarskis, C.R. Scafe, G. Sherlock, G. Binkley, H. Jin, et al. 2000. Integrating functional genomic information into the *Saccharomyces cerevisiae* genome database. *Nucleic Acids Res.* 28:77–80.

Baum, P., C. Furlong, and B. Byers. 1986. Yeast gene required for spindle pole body duplication: homology of its product with $Ca^{2+}$-binding proteins. *Proc. Natl. Acad. Sci. USA.* 83:5512–5516.

Biggins, S., and M. Rose. 1994. Direct interaction between yeast spindle pole body components: Kar1p is required for Cdc31p localization to the spindle pole body. *J. Cell Biol.* 125:843–852.

Bullitt, E., M. Rout, J. Kilmartin, and C. Akey. 1997. The yeast spindle pole body is assembled around a central crystal of Spc42p. *Cell.* 89:1077–1086.

Byers, B. 1981. Multiple roles of the spindle pole bodies in the life cycle of *Saccharomyces cerevisiae*. *In* Molecular Genetics in Yeast. Vol. 16. D. von Wettstein, A. Stenderup, M. Kielland-Brandt, and J. Friis, editors. Munksgaard, Copenhagen. 119–133.

Byers, B., and L. Goetsch. 1974. Duplication of spindle plaques and integration of the yeast cell cycle. *Cold Spring Harb. Symp. Quant. Biol.* 38:123–131.

Byers, B., and L. Goetsch. 1975. Behavior of spindles and spindles plaques in the cell cyle and conjugation of *Saccharomyces cerevisiae*. *J. Bacteriol.* 124:511–523.

Castillo, A.R., J.B. Meehl, G. Morgan, A. Schutz-Geschwender, and M. Winey. 2002. The yeast protein kinase Mps1p is required for assembly of the integral spindle pole body component Spc42p. *J. Cell Biol.* 156:453–465.

Chial, H.J., and M. Winey. 1999. Yeast spindle pole body duplication defects suggest mechanisms of genomic instability. *Biol. Cell.* 91:439–450.

Donaldson, A.D., and J.V. Kilmartin. 1996. Spc42p: A phosphorylated component of the *S. cerevisiae* spindle pole body (SPB) with an essential function during SPB duplication. *J. Cell Biol.* 132:887–901.

Elliott, S., M. Knop, G. Schlenstedt, and E. Schiebel. 1999. Spc29p is a component of the Spc110p-subcomplex and is essential for spindle pole body duplication. *Proc. Natl. Acad. Sci. USA.* 96:6205–6210.

Giddings, T.H., Jr., E.T. O'Toole, M. Morphew, D.N. Mastronarde, J.R. McIntosh, and M. Winey. 2001. Using rapid freeze and freeze-substitution for preparation of yeast cells for electron microscopy and three-dimensional analysis. *Methods Cell Biol.* 67:27–42.

Guthrie, C., and G.R. Fink. 1991. Guide to yeast genetics and molecular biology. *In* Methods in Enzymology. Vol. 194. Academic Press, San Diego. 933 pp.

Hinchcliffe, E.H., and G. Sluder. 2001. "It takes two to tango:" understanding how centrosome duplication is regulated throughout the cell cycle. *Genes Dev.* 15:1167–1181.

Hunter, K.J., and H.E. Eipel. 1979. Microbial determination by flow cytometry. *J. Gen. Microbiol.* 113:369–375.

Kilmartin, J., S. Dyos, D. Kershaw, and J. Finch. 1993. A spacer protein in the *Saccharomyces cerevisiae* spindle pole body whose transcript is cell cycle regulated. *J. Cell Biol.* 123:1175–1184.

Kumar, A., S. Agarwa, J.A. Heyman, S. Matson, M. Heidtman, S. Piccirillo, L. Umansky, A. Drawid, R. Jansen, Y. Liu, et al. 2002. Subcellular localization of the yeast proteome. *Genes Dev.* 16:707–719.

Longtine, M.S., A. McKenzie, D.J. Demarini, N.G. Shah, A. Wach, A. Brachat, P. Philippsen, and J.R. Pringle. 1998. Additional modules for versatile and economical PCR-based gene deletion and modification in *Saccharomyces cerevisiae. Yeast.* 14:953–961.

McIntosh, E.M., T. Atkinson, R.K. Storms, and M. Smith. 1991. Characterization of a short, cis-acting DNA sequence that conveys cell cycle stage-dependent transcription in *Saccharomyces cerevisiae. Mol. Cell. Biol.* 11:329–337.

Moreland, R.B., G.L. Langevin, R.H. Singer, R.L. Garcea, and L.M. Hereford. 1987. Amino acid sequences that determine the nuclear localization of yeast histone 2B. *Mol. Cell. Biol.* 7:4048–4057.

O'Toole, E.T., M. Winey, and J.R. McIntosh. 1999. High-voltage electron tomography of spindle pole bodies and early mitotic spindles in the yeast *Saccharomyces cerevisiae. Mol. Biol. Cell.* 10:2017–2031.

Paoletti, A., M. Moudjou, M. Paintrand, J.L. Salisbury, and M. Bornens. 1996. Most of centrin in animal cells is not centrosome-associated and centrosomal centrin is confined to the distal lumen of centrioles. *J. Cell Sci.* 109:3089–3102.

Rose, M., and G. Fink. 1987. *KAR1*, a gene required for function of both intranuclear and extranuclear microtubules in yeast. *Cell.* 48:1047–1060.

Rose, M., F. Winston, and P. Hieter. 1990. Methods in Yeast Genetics–A Laboratory Course Manual. Cold Spring Harbor Laboratory Press, Cold Spring Harbor, NY. 198 pp.

Salisbury, J.L., K.M. Suino, R. Busby, and M. Springett. 2002. Centrin-2 is required for centriole duplication in mammalian cells. *Curr. Biol.* 12:1287–1292.

Schild, D., H. Ananthaswamy, and R. Mortimer. 1981. An endomitotic effect of a cell cycle mutation of *Saccharomyces cerevisiae. Genetics.* 97:551–562.

Schramm, C., C. Janke, and E. Schiebel. 2001. Molecular dissection of yeast spindle pole bodies by two hybrid, in vitro binding, and co-purification. *Methods Cell Biol.* 67:71–94.

Schutz, A.R., and M. Winey. 1998. New alleles of the yeast *MPS1* gene reveal multiple requirements in spindle pole body duplication. *Mol. Biol. Cell.* 9:759–774.

Sikorski, R.S., and P. Hieter. 1989. A system of shuttle vectors and yeast host stains for efficient manipulation of DNA in *Saccharomyces cerevisiae. Genetics.* 122: 19–27.

Spang, A., I. Courtney, U. Fackler, M. Matzner, and E. Schiebel. 1993. The calcium-binding protein division cycle 31 of *Saccharomyces cerevisiae* is a component of the half bridge of the spindle pole body. *J. Cell Biol.* 123:405–416.

Spang, A., I. Courtney, K. Grein, M. Matzner, and E. Schiebel. 1995. The Cdc31p-binding protein Kar1p is a component of the half bridge of the yeast spindle pole body. *J. Cell Biol.* 128:863–877.

Spellman, P.T., G. Sherlock, M.Q. Zhang, V.R. Iyer, K. Anders, M.B. Eisen, P.O. Brown, D. Botstein, and B. Futcher. 1998. Comprehensive identification of cell cycle-regulated genes of the yeast *Saccharomyces cerevisiae* by microarray hybridization. *Mol. Biol. Cell.* 9:3273–3297.

Srivastava, A., and E.W. Jones. 1998. Pth1/Vam3p is the syntaxin homolog at the vacuolar membrane of *Saccharomyces cerevisiae* required for the delivery of vacuolar hydrolases. *Genetics.* 148:85–98.

Sullivan, D.S., S. Biggins, and M.D. Rose. 1998. The yeast centrin, Cdc31p, and the interacting protein kinase, Kic1p, are required for cell integrity. *J. Cell Biol.* 143:751–765.

Vallen, E., M. Hiller, T. Scherson, and M. Rose. 1992a. Separate domains of *KAR1* mediate distinct functions in mitosis and nuclear fusion. *J. Cell Biol.* 117:1277–1287.

Vallen, E., T.Y. Scherson, T. Roberts, K. van Zee, and M.D. Rose. 1992b. Asymmetric mitotic segregation of the yeast spindle pole body. *Cell.* 69:505–515.

Vallen, E., W. Ho, M. Winey, and M. Rose. 1994. Genetic interactions between *CDC31* and *KAR1*, two genes required for duplication of the microtubule organizing center in *Saccharomyces cerevisiae. Genetics.* 137:407–422.

Wigge, P.A., O.N. Jensen, S. Holmes, S. Soues, M. Mann, and J.V. Kilmartin. 1998. Analysis of the *Saccharomyces* spindle pole by matrix-assisted laser desorption/ionization (MALDI) mass spectrometry. *J. Cell Biol.* 141:967–977.

Winey, M., L. Goetsch, P. Baum, and B. Byers. 1991. *MPS1* and *MPS2*: novel yeast genes defining distinct steps of spindle pole body duplication. *J. Cell Biol.* 114:745–754.

Winey, M., A. Hoyt, C. Chan, L. Goetsch, D. Botstein, and B. Byers. 1993. *NDC1*: a nuclear periphery component required for yeast spindle pole body duplication. *J. Cell Biol.* 122:743–751.